New Geomagnetic Limits on the Photon Mass and on Long-Range Forces Coexisting with Electromagnetism

E. Fischbach,[1] H. Kloor,[1] R.A. Langel,[2,3] A.T.Y. Lui,[4] and M. Peredo[5]
[1]*Physics Department, Purdue University, West Lafayette, Indiana 47907*
[2]*Geodynamics Branch, Goddard Space Flight Center, Greenbelt, Maryland 20771*
[3]*Department of Earth and Atmospheric Sciences, Purdue University, West Lafayette, Indiana 47907*
[4]*Applied Physics Laboratory, Johns Hopkins University, Laurel, Maryland 20723*
[5]*Hughes/STX Corporation, Lanham, Maryland 20706*
(Received 29 March 1994)

A new geomagnetic limit on the photon mass m_γ is derived from an analysis of satellite measurements of the Earth's magnetic field $\vec{H}$. The primary effect of a nonzero photon mass is to generate an additional contribution to $\vec{H}$ resembling that from an external source. We find $m_\gamma \leq 8 \times 10^{-16}$ eV/c^2 $= 1 \times 10^{-48}$ g $= 4 \times 10^{-9}$ m^{-1}. The same data are also used to set new limits on long-range fields coexisting with electromagnetism.

PACS numbers: 14.70.Bh, 12.20.Fv, 91.25.Ga

It is well known that Maxwell's equations for classical electrodynamics can be obtained from a quantized theory in which fermions couple to photons whose mass m_γ is zero. Since both classical and quantum electrodynamics are strongly supported experimentally, it is tempting to conclude that the photon must in fact be massless. It can be shown, however, that a theory of massive quantum electrodynamics (where $m_\gamma \neq 0$) is fully consistent theoretically, and its predictions go over smoothly to those for the massless case as $m_\gamma \to 0$. Hence the possibility of a nonzero value of m_γ can never be completely excluded, and the results of a particular experiment only serve to set an upper bound on m_γ. It is worth noting that the situation is different for gravitons, the putative quanta of the gravitational field. As shown by van Dam and Veltman [1], the massless limit of a massive tensor theory of gravity does not correspond to general relativity, as might be expected naively, but rather to a theory containing a particular admixture of massless scalar and tensor fields. Since existing data exclude such an admixture, gravitons must be massless. However, a generalized Einstein theory combining massless and massive fields may be compatible with existing data, as discussed in Ref. [2], and this is analogous to the two-component electromagnetic theory discussed below.

The geomagnetic limit on m_γ is obtained by applying Schrödinger's observation [3] that when $m_\gamma \neq 0$ the Earth's magnetic field acquires an additional contribution which simulates the field due to an external source. It follows that one can derive an upper bound on m_γ by setting a limit on the contributions from such sources. (Although a more stringent bound on m_γ can be set by astrophysical arguments, these are necessarily indirect and hence are fraught with various uncertainties, as we discuss below.) The functional form of the additional component can be expressed in terms of the Earth's dipole field $\vec{H}_0(\vec{r})$,

$$\vec{H}_0(\vec{r}) = (1/r^3)[3(\vec{m}\cdot\hat{\mathbf{r}})\hat{\mathbf{r}} - \vec{m}], \quad (1)$$

where $\vec{m}$ is the dipole moment and $r = 0$ at the center of the dipole. It can be shown that when $m_\gamma \neq 0$, $\vec{H}_0(\vec{r})$ in Eq. (1) is replaced by [3–5]

$$\vec{H}(\vec{r}) = \vec{H}_0 e^{-x}(1 + x + x^2/3) - x^2 e^{-x}(2\vec{m}/3r^3), \quad (2)$$

where $x = r/\lambda$ and $\lambda = \hbar/m_\gamma c$ is the Compton wavelength of the (massive) photon. From Eq. (2) it follows that there are two distinct consequences of a nonzero photon mass which are relevant for the Earth's magnetic field: (a) The r dependence of the dipole contribution proportional to $\vec{H}_0$ changes and (b) an additional term parallel to the dipole direction appears. Since the latter contribution has the same angular dependence as that which would arise (for massless photons) from an external source, it represents a signal which is easier to study experimentally. Let $\vec{H}_{\rm ext}$ denote the apparent external magnetic field that remains after known effects from charges and currents are removed. The experimental quantity of interest is the ratio [4]

$$\kappa = \frac{(\vec{H}_{\rm ext}\cdot\hat{\mathbf{m}})_{\rm equator}}{(\vec{H}_{\rm dipole}\cdot\hat{\mathbf{m}})_{\rm equator}} \equiv \frac{H_{\rm ext}}{H_{\rm D.E.}}, \quad (3)$$

where $\vec{H}_{\rm dipole}$ is the term with the factor $[3(\vec{m}\cdot\hat{\mathbf{r}})\hat{\mathbf{r}} - \vec{m}]$ in $\vec{H}$. It follows from Eqs. (2) and (3) that κ is given by

$$\kappa = 2x^2(3 + 3x + x^2)^{-1}. \quad (4)$$

At the equator $x = (m_\gamma c/\hbar)R_\oplus$, where $R_\oplus = 6.38 \times 10^6$ m, and hence by combining Eq. (4) with an experimental bound on κ, one can infer a limit on m_γ. Goldhaber and Nieto (GN) [4] were the first to utilize satellite data for the Earth's magnetic field to set a bound on m_γ, and subsequently, Davis *et al.* [6] applied this formalism to analyze data on Jupiter's magnetic field obtained by Pioneer-10.

Since the publication of the GN results [4], much progress has been made in measurements of both the near-Earth field and of the fields due to magnetospheric sources. The latter are the cause of the true near-Earth

0031-9007/94/73(4)/514(4)$06.00

fields of external origin which would mimic the effect of $m_\gamma \neq 0$. As shown in Fig. 1, the net component of the external field along $\hat{m}$ can conveniently be divided into four contributions: $H^{(1)}$, arising from magnetopause currents (excluding those associated with the return path of the magnetotail currents); $H^{(2)}$, arising from magnetotail currents (including return currents); $H^{(3)}$, the equatorial ring current; and $H^{(4)}$, the field-aligned currents. All of these vary with time or, equivalently, with magnetic activity which is here measured by an index called *Dst* [7]. Magnetically quiet conditions correspond to a *Dst* value in the range 0 to -25 nT (1 nT$= 10^{-5}$ G). Since any field arising from $m_\gamma \neq 0$ will not vary with time, or with magnetic activity, attention is restricted to the values of $H^{(1)}, \ldots, H^{(4)}$ when *Dst* is in this range.

To understand how these fields are extracted from satellite data, note that in the absence of the solar wind the Earth's magnetic field would extend to infinity. The effect of the solar wind is to confine the field to a volume (the magnetosphere) with surface, the magnetopause, as shown in Fig. 1. The fields of interest, in addition to the dipole field, include those arising from the permanent presence of charged particles trapped in the magnetosphere. Using satellite data collected throughout the magnetosphere, i.e., for distances $r > 4R_\oplus$ from the center of the Earth, empirical models of these fields (and hence of the underlying currents) have been constructed by several authors, as discussed below. These models can then be used to predict the magnetic fields produced by these current systems at $r = R_\oplus$ where κ in Eq. (3) is defined.

Consider first the contribution from $H^{(3)}$ which, as noted above, arises from the ring current. The charges undergo drift motions in the magnetospheric environment and contribute to electric currents in space, which in turn generate $H^{(3)}$. The volume current density $\vec{j}_\perp$ perpendicular to the local magnetic field $\vec{H}$ is given by [8]

$$\vec{j}_\perp = \frac{\vec{H}}{H^2} \times \left[\vec{\nabla} P_\perp - (P_\parallel - P_\perp) \frac{(\vec{H} \cdot \vec{\nabla})\vec{H}}{H^2} \right], \qquad (5)$$

where $P_\parallel$ ($P_\perp$) is the component of the pressure tensor parallel (perpendicular) to the magnetic field. The magnitude of the term $(\vec{H} \cdot \vec{\nabla})\vec{H}/H^2$ gives the inverse of the radius of the magnetic field-line curvature. Assuming that the field-line curvature can be well represented by a dipole, which is reasonable for the quiet-time ring current, it follows from Eq. (5) that $\vec{j}_\perp$ can be determined from measurements of the magnetic field and the ring current particle population (which gives $P_\parallel$ and $P_\perp$) [9].

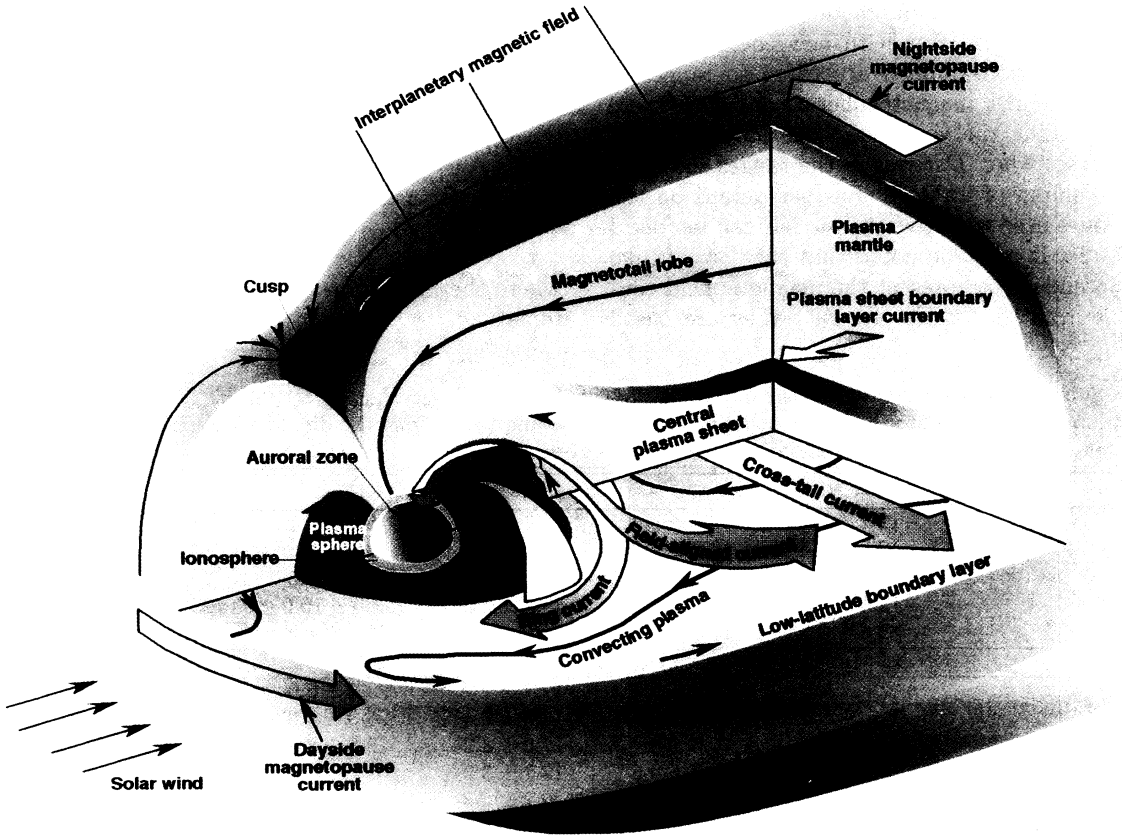

FIG. 1. Dominant space plasma current systems shown in a "cut-away" view of the Earth's magnetosphere.

Measurements of the ring current magnetic field and particle content from 16 orbits of the Charge Composition Explorer spacecraft, chosen to represent quiet geomagnetic periods, were used to compute the volume current density of the ring current along the satellite trajectory. The current density was then used to compute $H^{(3)}$ at the surface of the Earth, by assuming that the ring current flows symmetrically in a ring around the Earth, which is justifiable for quiet-time conditions. A linear fit of the component of $H^{(3)}$ along $\vec{m}$ as a function of the corresponding Dst value for each orbit gives

$$H^{(3)} = 11.6 \pm 1.3 \text{ nT} - (0.429 \pm 0.149)Dst, \quad (6)$$

where Dst is in nT, and the uncertainties are 1σ bounds. In Eq. (6) the sign convention is that a positive value of $H^{(3)}$ describes a field parallel to the dipole direction $\vec{m}$, which itself points approximately north to south at the center of the Earth.

Consider next the contributions from $H^{(1)}$, $H^{(2)}$, and $H^{(4)}$. Tsyganenko [10] has developed models with separate parametrizations for $H^{(2)}$, $H^{(3)}$, and $H^{(1)} + H^{(4)}$. We will use the results in Eq. (6) for the near-Earth value of $H^{(3)}$, since we consider this to be more accurate than that based on the Tsyganenko models. To obtain $H^{(2)}$ and the sum $H^{(1)} + H^{(4)}$, new versions of the Tsyganenko models [10] were used which are derived from an expanded data set [11]. Several of the models were studied and provide comparable results; the specific values quoted below correspond to the model labeled T87W in Appendix A of Ref. [12], but with new coefficients derived from observations binned according to ranges of the Dst index. Quiet magnetospheric conditions were selected by choosing the versions of the model derived from observations when Dst was in the ranges shown in the leftmost column of Table I. Further details on the fitting procedure used to derive the models can be found in Refs. [10–12]. It must be noted that the Tsyganenko models are intended to represent the magnetic field configuration far from the Earth. As such they are based on observations inside the magnetosphere but outside a radius $4R_\oplus$, and hence our estimate at $R_\oplus$ is based on an extrapolation of the model.

Table I summarizes the calculated values of $H^{(1)}, \ldots, H^{(4)}$ along $\hat{\mathbf{m}}$, as well as the actual measured near-Earth fields. These have been inferred by Sabaka and Baldwin [13] from data obtained by the Magsat and POGO satellites, together with surface magnetic observatory data, and are quoted for both noon and midnight as a function of Dst. Table I shows that the agreement between the measured and calculated values of the external magnetic field is excellent, particularly as it extends over a range of Dst values for both the noon and midnight results. In the notation of Ref. [5] and Eq. (3), the difference $H_{\text{ext}} \equiv H_{\text{meas}} - H_{\text{calc}}$ between the measured and calculated fields represents the "external" field component which could be attributed to a nonzero photon mass. Taking a weighted average of the results in Table I gives $H_{\text{ext}} = 0.4 \pm 2.2$ nT. Notwithstanding the agreement between the measured and calculated values of the fields, some caution is necessary in applying the results in Table I. To start with, use of the ring current model of Lui *et al.* [9] for $H^{(3)}$, in place of the $H^{(3)}$ arising from the Tsyganenko model, may lead to a model which is not completely consistent internally. In addition, we note the danger of extrapolating any of these models to regions outside of those where the input data for the model were obtained. Note that this caution applies as well to the earlier results of Refs. [3,4,6]. Finally we note that there is a small systematic difference of approximately 2.4 nT between the noon and midnight determinations of H_{ext}, but this is well within the quoted errors. From an analysis of possible errors arising from all of these sources it is estimated that they contribute a possible 1σ systematic uncertainty of ± 10 nT. Hence the final result for H_{ext} is

$$H_{\text{ext}} = 0.4 \pm 2.2(\text{stat}) \pm 10(\text{syst}) \text{ nT}, \quad (7)$$

where the first error is statistical and the second is systematic.

TABLE I. Summary of final results for the difference $H_{\text{ext}} = H_{\text{meas}} - H_{\text{calc}}$. $H_{\text{calc}} = H^{(1)} + H^{(2)} + H^{(3)} + H^{(4)}$, where all quantities (in units of nT) denote the components of the corresponding fields along the dipole direction. N and M denote noon and midnight, respectively. Note that some of the Dst ranges overlap.

Time/Dst	$H^{(1)} + H^{(4)}$	$H^{(2)}$	$H^{(3)}$	H_{calc}	H_{meas}	H_{ext}
N/0 to −5	-12.7 ± 3.8	15.8 ± 4.4	12.7 ± 1.7	15.8 ± 6.1	17.0 ± 2.0	1.2 ± 6.4
N/−5 to −10	-12.3 ± 2.4	16.0 ± 2.7	14.8 ± 2.4	18.5 ± 4.3	19.8 ± 2.0	1.3 ± 4.8
N/−5 to −15	-13.7 ± 4.4	17.2 ± 5.2	17.0 ± 3.2	20.5 ± 7.5	22.5 ± 2.0	2.0 ± 7.8
N/−15 to −20	-13.0 ± 6.9	17.7 ± 7.5	19.1 ± 3.9	23.8 ± 10.9	25.3 ± 2.0	1.5 ± 11.1
N/−15 to −25	-12.6 ± 3.2	17.4 ± 3.5	20.2 ± 4.3	25.0 ± 6.4	26.7 ± 2.0	1.7 ± 6.7
Noon weighted mean						1.5 ± 2.9
M/0 to −5	-8.9 ± 3.4	19.4 ± 5.7	12.7 ± 1.7	23.2 ± 6.9	22.5 ± 2.0	-0.7 ± 7.1
M/−5 to −10	-8.5 ± 2.2	20.0 ± 3.5	14.8 ± 2.4	26.3 ± 4.8	25.3 ± 2.0	-1.0 ± 5.2
M/−5 to −15	-9.7 ± 4	21.3 ± 6.7	17.0 ± 3.2	28.6 ± 8.4	28.0 ± 2.0	-0.6 ± 8.7
M/−15 to −20	-9.0 ± 6.3	21.7 ± 9.5	19.1 ± 3.9	31.8 ± 12.0	30.8 ± 2.0	-1.0 ± 12.2
M/−15 to −25	-8.6 ± 2.9	21.6 ± 4.5	20.2 ± 4.3	33.2 ± 6.9	32.2 ± 2.0	-1.0 ± 7.2
Midnight weighted mean						-0.9 ± 3.2
N+M Weighted mean						0.4 ± 2.2

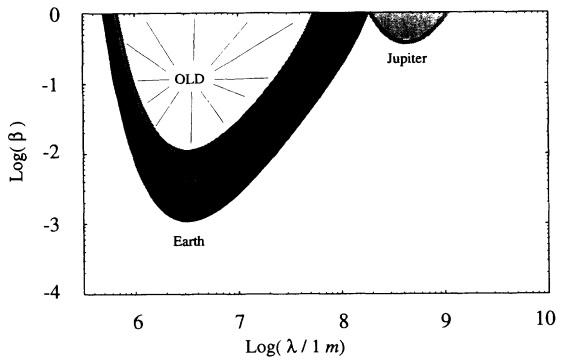

FIG. 2. Exclusion plot for $\beta = \beta(\lambda)$, where β and λ, respectively, characterize the strength and range of a new field. The shaded regions are excluded by the data at the 1σ level. Note that the new results provide the first nontrivial constraint on $\beta = \beta(\lambda)$ for the region around $\lambda \approx 10^8$ m. The data for Jupiter are obtained from Ref. [5].

From the earlier discussion recall that the effect of $m_\gamma \neq 0$ is to generate a field $\vec{H}_{\rm ext}$ along $-\hat{\mathbf{m}}$, which means that $\vec{H}_{\rm ext}$ and the dipole field point in the same direction at the equator. Using Eq. (7) the largest *negative* value that $\vec{H}_{\rm ext}$ can have (at the 1σ level) is $H_{\rm ext} = -11.8$ nT. To compute κ from Eq. (3) the value $H_{\rm D.E.} = 30\,573$ nT quoted in Ref. [14] is used. This gives

$$\kappa \leq 3.9 \times 10^{-4}. \tag{8}$$

Hence from Eq. (4),

$$\hbar/m_\gamma c \geq 3 \times 10^8 \text{ m},$$
$$m_\gamma \leq 8 \times 10^{-16} \text{ eV}/c^2 = 1 \times 10^{-48} \text{ g}. \tag{9}$$

The result for κ in Eq. (8) is a factor of 10 smaller than that obtained by GN [4]. Since $x = (m_\gamma c/\hbar)R_\oplus \approx (3\kappa/2)^{1/2}$, it follows that the limit on m_γ in Eq. (9) is approximately 3 times smaller than the GN value. Moreover, the new limit is only slightly less sensitive than that obtained from the Jupiter data [6], and could surpass the Jupiter value when refinements presently under way are completed. Although smaller limits on m_γ have been quoted based on astrophysical arguments, these are necessarily more uncertain. The smallest published limit is $m_\gamma \lesssim 3 \times 10^{-60}$ g quoted by Chibisov [15] from an analysis of magnetized interstellar gas. However, this bound must be interpreted with some caution, since it depends in a critical way on the applicability of the virial theorem, and on other dynamical assumptions, such as equilibrium of the interstellar gas.

As discussed in Refs. [5,16] the same data which constrain m_γ in a theory where the photon has a nonzero mass can also be used to constrain both the range λ and coupling strength β of a new field coexisting with conventional (massless) electrodynamics. The constants β and λ are defined [5,16] in terms of the effective static potential $V(r)$ for two test objects with charges $Q_1 e$ and $Q_2 e$, respectively ($e^2/\hbar c \approx 1/137$):

$$V(r) = \frac{Q_1 Q_2 e^2}{r}(1 + \beta e^{-r/\lambda}). \tag{10}$$

From Eq. (10) it is seen that β characterizes the strength of the new interaction in units of e^2, and λ is the Compton wavelength of the quantum of the new field. As shown in Refs. [5,16], an experimental upper bound on κ leads to a constraint on β and λ through the relation

$$\kappa = \frac{(2/3)(r/\lambda)^2 \beta e^{-r/\lambda}}{[1 + \beta e^{-r/\lambda}(1 + r/\lambda + r^2/3\lambda^2)]}. \tag{11}$$

An exclusion plot in the β-λ plane is shown in Fig. 2 corresponding to the new limit on κ quoted in Eq. (8). This limit provides the first nontrivial constraint on $\beta(\lambda)$ for values of λ near 10^8 m.

One of the authors (E.F.) wishes to acknowledge the support of the U.S. Department of Energy under Contract No. DE-AC02-76ER01428. H.K. is supported by a David Ross fellowship at Purdue University. R.A.L. would like to acknowledge the support of NASA RTOP 579-31-02, as well as the support furnished by the Department of Earth and Atmospheric Sciences at Purdue during his sabbatical. A.T.Y.L. is supported by National Science Foundation Grant No. ATM-9114316 to the Johns Hopkins University. The authors wish to thank Carrick Talmadge and Naren Shankar for helpful discussions.

[1] H. van Dam and M. Veltman, Nucl. Phys. **B22**, 397 (1970); Gen. Relativ. Gravitation **3**, 215 (1972). See also V.I. Zakharov, JETP Lett. **12**, 312 (1970).
[2] M. Kenmoku, Y. Okamoto, and K. Shigemoto, Phys. Rev. D **48**, 578 (1993).
[3] E. Schrödinger, Proc. Roy. Ir. Acad. A **49**, 135 (1943).
[4] A. S. Goldhaber and M. M. Nieto, Phys. Rev. Lett. **21**, 567 (1968); Rev. Mod. Phys. **43**, 277 (1971).
[5] H. Kloor, E. Fischbach, C. Talmadge, and G.L. Greene, Phys. Rev. D **49**, 2098 (1994). We follow the notation of this paper after substituting $\hat{\mathbf{z}}D \rightarrow \vec{m}$.
[6] L. Davis, A. Goldhaber, and M.M. Nieto, Phys. Rev. Lett. **35**, 1402 (1975).
[7] J. H. Allen and J. Feynman, *Review of Selected Geomagnetic Activity Indices,* Solar-Terrestrial Predictions Proceedings Vol. 2, edited by R.E. Donnelly (U.S. Department of Commerce, Environmental Research Laboratories, Boulder, 1979).
[8] E. N. Parker, Phys. Rev. **107**, 924 (1957).
[9] A.T.Y. Lui, R.W. McEntire, and S.M. Krimigis, J. Geophys. Res. **92**, 1402 (1987).
[10] N.A. Tsyganenko, Planet. Space Sci. **35**, 5 (1989); Space Sci. Rev. **54**, 75 (1990).
[11] M. Peredo *et al.*, Eos Trans. AGU **73**, 462 (1992); N.A. Tsyganenko *et al.*, Eos Trans. AGU **73**, 256 (1992).
[12] M. Peredo, D.P. Stern, and N.A. Tsyganenko, J. Geophys. Res. **98**, 15 343 (1993).
[13] T.J. Sabaka and R.T. Baldwin, Hughes/STX Report HSTX/G&G, 1993 (unpublished), p. 9302.
[14] R.A. Langel and R.H. Estes, J. Geophys. Res. **90**, 2495 (1985).
[15] G.V. Chibisov, Sov. Phys. Usp. **19**, 624 (1976).
[16] D. Bartlett and S. Lögl, Phys. Rev. Lett. **61**, 2285 (1988).

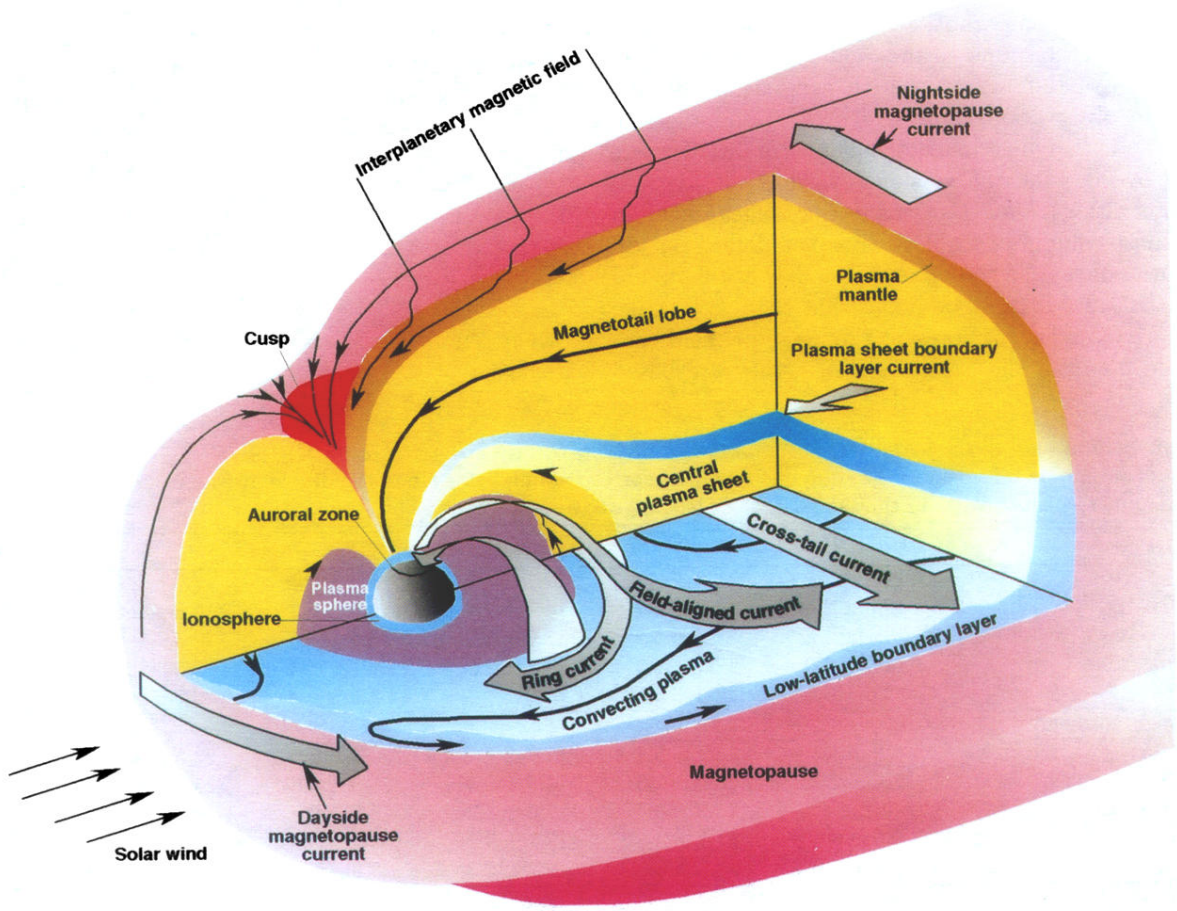

FIG. 1. Dominant space plasma current systems shown in a "cut-away" view of the Earth's magnetosphere.

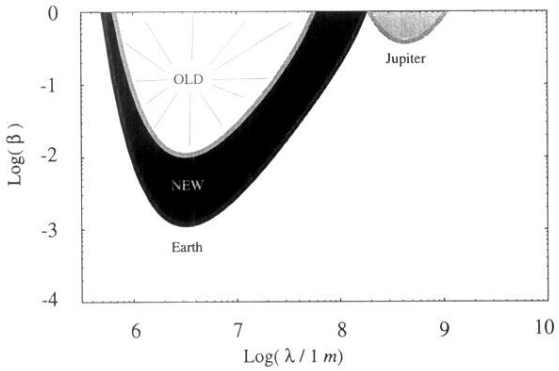

FIG. 2. Exclusion plot for $\beta = \beta(\lambda)$, where β and λ, respectively, characterize the strength and range of a new field. The shaded regions are excluded by the data at the 1σ level. Note that the new results provide the first nontrivial constraint on $\beta = \beta(\lambda)$ for the region around $\lambda \approx 10^8$ m. The data for Jupiter are obtained from Ref. [5].